

## 3DXRD and TotalCryst Geometry

Version 1.0.2

*H.F. Poulsen, S. Schmidt, J. Wright, H.O. Sørensen*

This note defines the geometry related to the 3DXRD methodology as implemented at ID11 at ESRF. It is mainly an extension of the work presented in the book by Poulsen [1] and the more recent summary in the book by Banhardt [2]. The reader is expected to be familiar with single crystal diffraction.

The note serve as a standard for the geometry in a suite of programs available under the TotalCryst umbrella<sup>1</sup> such as FABLE, near- and farfield simulators, Fabian, ImageD11, GrainSpotter, Grainsweeper, and the Monte Carlo routines for grain mapping. For historic reasons, the representation within the program may not always follow the standard, but should apply to the user interfaces.

A few comments on typography: vectors are written with underline, matrices and quaternions in bold<sup>2</sup> and tensors with no special fonts (but distinguishable by their suffices).

### 1 The basic 3DXRD set-up

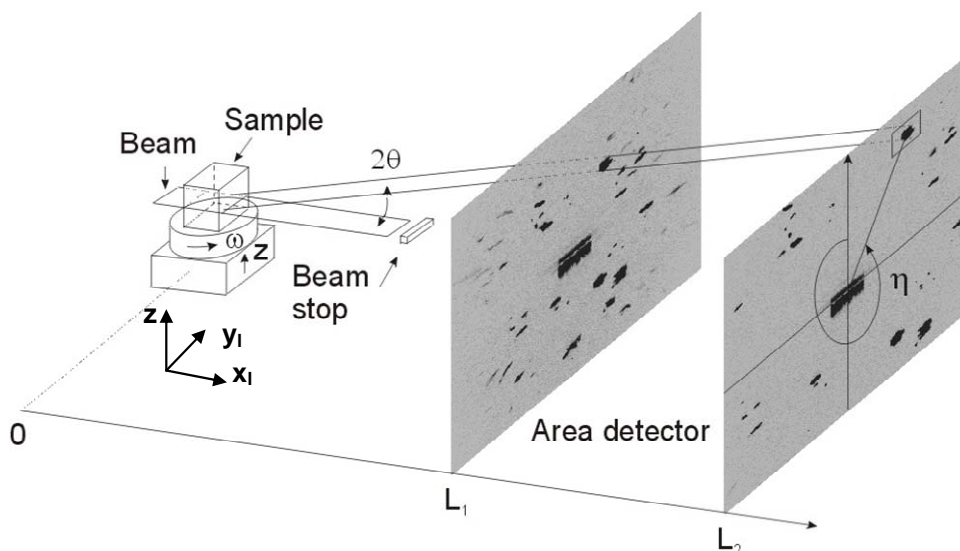


**Figure 1.1**

Sketch of the 3DXRD principle for the case of the incoming monochromatic beam being focused in one dimension. The Bragg angle  $2\theta$ , the rotation angle  $\omega$  and the azimuthal angle  $\eta$  are indicated for the diffracted beam arising from one grain of a coarse-grained specimen, and for two settings of the area detector. The axes for the laboratory co-ordinate system are also shown.

<sup>1</sup> See [www.totalcryst.dk](http://www.totalcryst.dk) and [fable.sourceforge.net](http://fable.sourceforge.net)

<sup>2</sup> Unfortunately Words doesn't allow for bold face in the equations.

The 3DXRD method is an extension of the “rotation method” known from single crystal crystallography. The basic set-up is sketched in Fig 1.1. A monochromatic x-ray beam is constrained to a suitable cross-section by means of focusing and/or the use of absorbing slits. This beam may illuminate the whole sample, or only parts of it.

The sample is mounted on a goniometer. The prototypical set-up considered in this version of the document comprises only one rotation stage, an  $\omega$ -stage rotating around an axis perpendicular to the incoming beam, see Fig 1.1. Furthermore, for convenience, we shall in the text assume the  $\omega$ -axis is vertical, although this restriction is not required by the algebra. However, we will provide equations for more general rotations for use e.g. in connection with a four circle or a double tilt below the  $\omega$ -stage. There are no translations.

Any part of the illuminated structure, which fulfils the Bragg condition, will generate a diffracted beam. This beam is transmitted through the sample and probed by one or more 2D detectors. Essential to 3DXRD is the idea to use such detectors to mimic a 3D detector, similar to the ones used in particle physics. This can be done in two ways. Firstly, by positioning several 2D detectors at different distances to the centre-of-rotation,  $L$ , and exposing these either simultaneously (many detectors are semi-transparent to hard x-rays) or subsequently. Secondly, by acquiring images with one 2D detector positioned at several distances to the rotation axis, as illustrated in Fig 1.1.

To probe the complete structure, and not just the part that happens to fulfil the Bragg condition, the sample is rotated around one axis – the  $\omega$  axis. Hence, exposures are made for equi-angular settings of  $\omega$  with a step of  $\Delta\omega$ . To provide a uniform sampling the sample is rotated by  $\Delta\omega$  during each exposure. To avoid confusion of terms in the following  $\Delta\omega$  is termed the “oscillation range”. We shall adapt the convention that the omega range defined is the total range: e.g. a range of [0 10] in 10 steps imply that acquisitions are made around the points 0.5, 1.5 , ..., 9.5 – in each case while rotating by  $\pm 0.5$  degree around the nominal value. *This should be enforced in the specs macro: sweepscan etc.*

The azimuthal angle  $\eta$  (see Fig 1.1) is defined to be positive in the cw direction when looking downstream – from sample towards detector – and to be 0 pointing upwards.

With the detectors available, experience has proven two complementary detector configurations to be of particular use. Depending on the issue at hand, they may be used on a stand-alone basis or they can be combined.

*Near-field configuration:* A detector with a high spatial resolution positioned close to the specimen. Data acquisition may or may not be repeated at several distances (say 3 settings of  $L$  in the range of 1-10 mm). The angular resolution is relatively low, implying that the diffraction patterns are not influenced by any elastic strain, as the associated angular perturbations are too small to be observed. Hence, only spatial and orientation degrees of freedom are probed.

*Far-field configuration:* A detector with a low spatial resolution positioned at a fixed distance to the specimen (not shown in Fig 1.1). The distance is optimised such that the full diffraction pattern appears in the images (say  $L = 400$  mm at 50 keV). The diffraction spots now appear on a set of rings – the Debye-Scherrer rings well known from powder diffraction. In this case

the spatial degrees of freedom are to a large extent integrated out, whilst the angular resolution is medium.

The formalism developed below works for all distances and allows the plane of the detectors to be tilted with respect to the incoming beam.

The formalism developed below is subject to the following basic assumptions:

- The beam divergence and the energy band width is neglected
- Kinematical scattering

For more information, see Refs 1 and 2.

## 2 Diffraction geometry

The algebra for associating diffraction observations with reciprocal space is well described for single crystals. The polycrystal case differs by the need for one extra coordinate system since the sample and the grains are separate objects. In the following equations describing a single scattering event are derived. Mainly the single crystal formalism of Busing and Levy [3] is followed as close as possible<sup>3</sup>, but for a number of equations alternative – but equivalent - expressions are given, as used by the various programs in the full package. For reasons of simplicity, the relevant part of the sample is assumed fully illuminated at all  $\omega$ -settings.

### The laboratory and rotated coordinate systems

We first consider **the basic set-up** shown in Fig 1 with only one rotation axis, which is directed perpendicular to the incoming beam. In this case we define the laboratory system  $(\hat{x}_l, \hat{y}_l, \hat{z}_l)$  as having  $\hat{x}_l$  pointing along the incoming beam,  $\hat{y}_l$  transverse to it in the horizontal plane and  $\hat{z}_l$  positive upwards, parallel to the  $\omega$  rotation axis. Furthermore,  $(x_l, y_l) = (0, 0)$  along the  $\omega$ -rotation axis. The definition of  $z_l = 0$  is made by means of a reference beam of infinitesimal size.

In this system the direction of the diffracted ray can be parameterised by the Bragg angle  $\theta$  and the azimuthal angle  $\eta$ , both defined in Fig 1.1. Notably  $\eta$  is defined positively in the cw direction, when viewed along the beam direction from the sample towards the detector and  $\eta=0$  when pointing upwards (in the positive direction of  $\hat{z}_l$ ).

Next, we define  $\omega$  positive ccw when viewed along the z-axis from the top of the instrument. Then

$$\begin{pmatrix} x_l \\ y_l \\ z_l \end{pmatrix} = \Omega \begin{pmatrix} x_\omega \\ y_\omega \\ z_l \end{pmatrix} = \begin{pmatrix} \cos(\omega) & -\sin(\omega) & 0 \\ \sin(\omega) & \cos(\omega) & 0 \\ 0 & 0 & 1 \end{pmatrix} \begin{pmatrix} x_\omega \\ y_\omega \\ z_l \end{pmatrix}. \quad (2.1)$$

---

<sup>3</sup> However, the sign convention for  $\omega$  used here is opposite to the one used in [3].

The coordinates  $(x_\omega, y_\omega, z_l)$  refer to the rotated system, which is rigidly attached to the  $\omega$  turntable. This coordinate system is identical to the sample system, except if the user wants to redefine the latter using a matrix  $\mathbf{S}$ , see below.

We next consider a **more generalised goniometer**. Following Busing-Levy we shall operate with 3 rotations, namely an outer  $\omega$ -rotation stage (rotating around the  $z$ -axis), a  $\chi$ -rotation, and an innermost  $\phi$ -stage. The combined rotation is given by

$$\begin{pmatrix} x_l \\ y_l \\ z_l \end{pmatrix} = \Gamma \begin{pmatrix} x_\omega \\ y_\omega \\ z_l \end{pmatrix} = \Omega X \Theta \begin{pmatrix} x_\omega \\ y_\omega \\ z_l \end{pmatrix}. \quad (2.2)$$

This definition can be used to handle e.g. a Eulerian cradle, a Kappa-goniometer or a double-tilt above the  $\omega$ -axis. We shall leave the exact definition of  $\mathbf{X}$  and  $\Theta$  to the user. We will assume that the  $\omega$  rotation is used for scanning/oscillating during actual data acquisition, and this axis is perpendicular to the incident beam.

### Detector coordinate systems

The detector read-out is in a pixel coordinate system. Different detector systems use different conventions for how to flip the image and where to put the origin. We here define our own standard convention  $(y_{\text{raw}}, z_{\text{raw}})$ , which is used in equations below. This is a regular grid defined in pixels, as shown in Figure 2.1

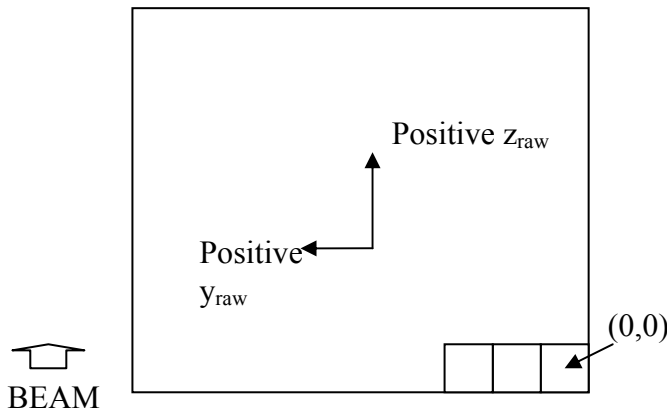


**Figure 2.1.** Definition of detector pixel coordinate system, see text.

Hence, for the detector plane normal parallel to the beam,  $y_{\text{raw}}$  is parallel to  $\hat{y}_l$  and  $z_{\text{raw}}$  is parallel to  $\hat{z}_l$ . We define  $(0,0)$  as corresponding to the centre of the pixel in the lower right corner of the image. This implies that the border of the detection area will have half-integer values.

The detector may be associated with spatial distortion, as given by the operator  $SC$ . We define  $(y_{\text{det}}, z_{\text{det}})$  to represent the corrected system:

$$(y_{\text{det}}, z_{\text{det}}) = SC((y_{\text{raw}}, z_{\text{raw}})) \quad (2.3)$$

The detector plane normal may be tilted with respect to the incoming beam. We define

$\phi_x$ : Tilt of detector around x (pos ccw around x: right-hand system)

$\phi_y$ : Tilt of detector around y (pos ccw around y: right-hand system)

$\phi_z$ : Tilt of detector around z (pos ccw around z: right-hand system)

Correspondingly we have rotation matrices  $\mathbf{R}^X$ ,  $\mathbf{R}^Y$  and  $\mathbf{R}^Z$ :

$$\mathbf{R}^X = \begin{pmatrix} 1 & 0 & 0 \\ 0 & \cos(\phi_x) & -\sin(\phi_x) \\ 0 & \sin(\phi_x) & \cos(\phi_x) \end{pmatrix}; \mathbf{R}^Y = \begin{pmatrix} \cos(\phi_y) & 0 & \sin(\phi_y) \\ 0 & 1 & 0 \\ -\sin(\phi_y) & 0 & \cos(\phi_y) \end{pmatrix}; \mathbf{R}^Z = \begin{pmatrix} \cos(\phi_z) & -\sin(\phi_z) & 0 \\ \sin(\phi_z) & \cos(\phi_z) & 0 \\ 0 & 0 & 1 \end{pmatrix}; \quad (2.4)$$

Furthermore we use the convention that the detector system is rotated with respect to the laboratory system by <sup>4</sup>

$$\mathbf{R} = \mathbf{R}^X \mathbf{R}^Y \mathbf{R}^Z. \quad (2.5)$$

We can now express the connection between a point on the detector as defined by pixel coordinates ( $y_{\text{det}}$ ,  $z_{\text{det}}$ ) and the corresponding point ( $x'$ ,  $y'$ ,  $z'$ ) in the laboratory system

$$\begin{pmatrix} x' \\ y' \\ z' \end{pmatrix} = \begin{pmatrix} L \\ 0 \\ 0 \end{pmatrix} + \mathbf{R} \begin{pmatrix} 0 \\ P_y(y_{\text{det}} - y_{\text{det}}(0)) \\ P_z(z_{\text{det}} - z_{\text{det}}(0)) \end{pmatrix} \quad (2.6)$$

Here by definition ( $y_{\text{det}}(0)$ ,  $z_{\text{det}}(0)$ ) are the pixel coordinates for the reference beam (the incident ray passing through  $(x_1, y_1, z_1) = (0,0,0)$ ),  $P_i$  is the pixelsize in the two directions, and  $L$  is the distance from center-of-rotation to the point where the incident ray hits the detector.

### Diffraction

The scattering vector associated with the diffraction event is denoted  $\underline{\mathbf{G}}$ . To describe its relationship with reciprocal space we need five Cartesian coordinate systems: the laboratory system, the omega-system, the rotated system, the sample system, and the Cartesian grain system. These are identified by subscripts  $l$ ,  $\omega$ ,  $\gamma$ ,  $s$  and  $c$ , respectively. The former three have already been defined. Hence, the scattering vector transforms as  $\underline{\mathbf{G}}_l = \underline{\mathbf{\Omega}} \underline{\mathbf{G}}_\omega = \underline{\mathbf{\Gamma}} \underline{\mathbf{G}}_\gamma$ . (in case of only one rotation axis:  $\underline{\mathbf{\Gamma}} = \underline{\mathbf{\Omega}}$ ).

The sample system is fixed with respect to the sample, as defined *a priori* by the experimentalist. As an example, in metallurgy the sample coordinates are typically defined by the rolling, transverse and normal directions of a rolled sheet (RD, TD, ND). The orientation of the sample on the  $\omega$  turntable is given by the  $\mathbf{S}$  matrix:  $\underline{\mathbf{G}}_\gamma = \mathbf{S} \underline{\mathbf{G}}_s$ . By default  $\mathbf{S} = \mathbf{I}$ , the identity matrix.

---

<sup>4</sup> Notably experience shows, that the order in which  $\mathbf{R}^X$ ,  $\mathbf{R}^Y$  and  $\mathbf{R}^Z$  appears is important even for relatively small tilts.

The crystallographic orientation of a grain with respect to the sample is represented by  $\mathbf{U}^5$ ,  $\underline{\mathbf{G}}_s = \mathbf{U}\underline{\mathbf{G}}_c$ . where index c refers to a Cartesian grain system  $(\hat{x}_c, \hat{y}_c, \hat{z}_c)$ . This is fixed with respect to the reciprocal lattice  $(\underline{a}^*, \underline{b}^*, \underline{c}^*)$  in the grain. We use the convention that  $\hat{x}_c$  is parallel to  $\underline{a}^*$ ,  $\hat{y}_c$  is in the plane of  $\underline{a}^*$  and  $\underline{b}^*$ , and  $\hat{z}_c$  is perpendicular to that plane. Let  $\underline{\mathbf{G}}$  be represented in the reciprocal lattice system by the integer Miller indices  $\underline{\mathbf{G}}_{hkl} = (h, k, l)^t$ . The correspondence between the Cartesian grain system and reciprocal space is then given by the  $\mathbf{B}$  matrix:  $\underline{\mathbf{G}}_c = \mathbf{B} \underline{\mathbf{G}}_{hkl}$ , with

$$\mathbf{B} = \begin{pmatrix} a^* & b^* \cos(\gamma^*) & c^* \cos(\beta^*) \\ 0 & b^* \sin(\gamma^*) & -c^* \sin(\beta^*) \cos(\alpha) \\ 0 & 0 & c^* \sin(\beta^*) \sin(\alpha) \end{pmatrix} \quad (2.7)$$

and<sup>6</sup>

$$\cos(\alpha) = \frac{\cos(\beta^*) \cos(\gamma^*) - \cos(\alpha^*)}{\sin(\beta^*) \sin(\gamma^*)}. \quad (2.8)$$

Here  $(a, b, c, \alpha, \beta, \gamma)$  and  $(a^*, b^*, c^*, \alpha^*, \beta^*, \gamma^*)$  symbolize the lattice parameters in direct and reciprocal space, respectively.

With these definitions we have

$$\underline{\mathbf{G}}_l = \Gamma \mathbf{SUB} \underline{\mathbf{G}}_{hkl}. \quad (2.9)$$

At times it is relevant to operate with normalised scattering vectors instead. Let  $\underline{u} = \underline{\mathbf{G}}_l / \|\underline{\mathbf{G}}_l\|$ ,  $\underline{y} = \underline{\mathbf{G}}_s / \|\underline{\mathbf{G}}_s\|$  and  $\underline{h} = \frac{B \underline{\mathbf{G}}_{hkl}}{\|B \underline{\mathbf{G}}_{hkl}\|}$ . Then

$$\underline{u} = \Gamma S \underline{y} = \Gamma S U \underline{h} = \begin{pmatrix} -\sin(\theta) \\ -\cos(\theta) \sin(\eta) \\ \cos(\theta) \cos(\eta) \end{pmatrix}. \quad (2.10)$$

For completeness we mention that Bragg's law provides an alternative way to determine the norm of the  $\underline{\mathbf{G}}$ -vectors. Using a formalism that includes  $2\pi$  in the reciprocal space definition, the corresponding equation for  $\underline{h}$  is

$$\begin{pmatrix} h_1 \\ h_2 \\ h_3 \end{pmatrix} = \frac{\lambda}{4\pi \sin(\theta)} B \begin{pmatrix} h \\ k \\ l \end{pmatrix}. \quad (2.11)$$

<sup>5</sup> In the texture community it is customary to operate with  $\mathbf{g} = \mathbf{U}^{-1}$ . Notably this  $\mathbf{g}$  is not related to the metric  $\mathbf{g}$  in Eq. 2.22 nor the metric in Eq. 3.4.

<sup>6</sup> There is an error in this formula in the book by Poulsen [1].

## Forward projection

Let the diffraction event take place at position  $(x_l, y_l, z_l)$  in the sample system and be associated with a certain orientation  $\mathbf{U}$ . Assume further we know  $\mathbf{X}$  and  $\Theta$ , the spacegroup, the lattice parameters (and therefore  $\mathbf{B}$ ) and the x-ray wavelength. The task at hand is then to find the detector coordinates for the diffraction spot associated with a set of Miller indices  $\underline{G}_{hkl}$ .

We may proceed as follows. For each  $\underline{G}_{hkl}$  first we find  $\underline{G}_\omega$ . The  $\omega$ -position at which the diffraction condition is fulfilled is then given by

$$\sin(\theta) = -u_1 = -[\mathbf{\Omega G}_\omega]_1. \quad (2.12)$$

with  $\sin(\theta)$  defined by Braggs law. This is a quadratic equation for determination of  $\omega$  given  $\underline{G}_\omega$  and  $\underline{h}$ . The two possible solutions are<sup>7</sup>

$$\cos \omega = \frac{ac \pm b\sqrt{D}}{a^2 + b^2}, \quad \sin \omega = \frac{bc \mp a\sqrt{D}}{a^2 + b^2}. \quad (2.13)$$

where

$$a = \frac{G_{\omega,1}}{|G_\omega|}, b = \frac{-G_{\omega,2}}{|G_\omega|}, c = \frac{\cos(2\theta) - 1}{\sqrt{2 - 2\cos(2\theta)}}, \quad \text{and} \quad \sqrt{D} = a^2 + b^2 - c^2. \quad (2.14)$$

Depending on  $\omega$ -range 0, 1 or 2 of these solutions may be real.

Knowing  $\mathbf{\Omega}$  we can compute  $\underline{G}_l$  and  $\underline{u}$ . In the **case of an untilted detector** we have

$$\begin{aligned} P_Y(y_{\text{det}} - y_{\text{det}}(0)) &= y_l - (L - x_l) \tan(2\theta) \sin(\eta) = y_l + \frac{(L - x_l) \tan(2\theta)}{\cos(\theta)} u_2 = y_l + \frac{(L - x_l) \lambda}{2\pi \cos(2\theta)} G_{l,2}; \\ P_Z(z_{\text{det}} - z_{\text{det}}(0)) &= z_l + (L - x_l) \tan(2\theta) \cos(\eta) = z_l + \frac{(L - x_l) \tan(2\theta)}{\cos(\theta)} u_3 = z_l + \frac{(L - x_l) \lambda}{2\pi \cos(2\theta)} G_{l,3} \end{aligned} \quad (2.15)$$

In **case of a tilted detector**, in the laboratory system the detection event takes place at

$$\begin{pmatrix} x' \\ y' \\ z' \end{pmatrix} = \begin{pmatrix} x_l \\ y_l \\ z \end{pmatrix} + t\vec{v} = \begin{pmatrix} L \\ 0 \\ 0 \end{pmatrix} + R \begin{pmatrix} 0 \\ P_Y(y_{\text{det}} - y_{\text{det}}(0)) \\ P_Z(z_{\text{det}} - z_{\text{det}}(0)) \end{pmatrix} \quad (2.16)$$

Here  $\underline{v}$  is the unit directional vector:

<sup>7</sup> The derivation of Eqs. 2.13 and 2.14 is due to S. Schmidt.

$$\underline{y} = \begin{pmatrix} \cos(2\theta) \\ -\sin(2\theta)\sin(\eta) \\ \sin(2\theta)\cos(\eta) \end{pmatrix}. \quad (2.17)$$

We want to solve these three row equations in (2.16) for  $t$ ,  $y_{det}$ ,  $z_{det}$ . The solution is

$$t = \frac{R_{11}(L - x_l) - R_{21}y_l - R_{31}z_l}{R_{11}v_1 + R_{21}v_2 + R_{31}v_3}. \quad (2.18)$$

From which we find:

$$\begin{aligned} P_y(y_{det} - y_{det}(0)) &= R_{12}((x_l - L) + tv_1) + R_{22}(y_l + tv_2) + R_{32}(z_l + tv_3) \\ P_z(z_{det} - z_{det}(0)) &= R_{13}((x_l - L) + tv_1) + R_{23}(y_l + tv_2) + R_{33}(z_l + tv_3). \end{aligned} \quad (2.19)$$

*Flipping:* The above equations assume that the detector read-out is not flipped with respect to the standard laboratory system. If flipping is needed, it should be performed just after the spatial distortion correction.

### Indexing<sup>8</sup>

A main task for 3DXRD programs is to index polycrystalline materials. Here we introduce some notation – as used primarily in the program ImageD11 – for the case of indexing a single crystal. We shall assume that the  $\mathbf{B}$  matrix is not a priori known.

For each spot on the detector we know  $\mathbf{\Omega}$ ,  $\mathbf{X}$  and  $\mathbf{\Theta}$  and as such we can determine  $\underline{\mathbf{G}}_y$ . Associating these with a set of Miller indices  $\underline{\mathbf{G}}_{hkl}$ , we have

$$\underline{\mathbf{G}}_y = \mathbf{\Theta}^{-1} \mathbf{X}^{-1} \mathbf{\Omega}^{-1} \underline{\mathbf{G}}_L = (\mathbf{UB}) \underline{\mathbf{G}}_{hkl}. \quad (2.20)$$

The process of indexing is then the process of determining  $(\mathbf{UB})$  or  $(\mathbf{UB})^{-1}$  so that  $\underline{\mathbf{G}}_{hkl}$  are simple integers.

To continue we introduce the metric tensor  $\mathbf{g} = (\mathbf{UB})^t(\mathbf{UB})$

$$\mathbf{g} = \begin{pmatrix} a^2 & ab \cos(\gamma) & ac \cos(\beta) \\ ab \cos(\gamma) & b^2 & bc \cos(\alpha) \\ ac \cos(\beta) & bc \cos(\alpha) & c^2 \end{pmatrix}. \quad (2.21)$$

The unit cell volume is given by the determinant of  $\mathbf{g}$ . Adding a “\*” to all symbols we get the same relations in reciprocal space with  $\mathbf{g}^* = \mathbf{g}^{-1}$ .

It turns out that (since  $\mathbf{U}^t = \mathbf{U}^{-1}$ )

$$\mathbf{g} = (\mathbf{UB})^t(\mathbf{UB}) = \mathbf{B}^t \mathbf{U}^t \mathbf{UB} = \mathbf{B}^t \mathbf{B} \quad (2.22)$$

---

<sup>8</sup> This section by J. Wright

Hence, knowing  $\mathbf{g}$  one can determine  $\mathbf{U}$  and  $\mathbf{B}$  by Cholesky decomposition [4] [Jon, more info here.](#)

### Implementation

We adapt the convention that all angles in user input/output are given in degrees. Linear dimensions will be specified in each module, but will preferably be in mm and  $\mu\text{m}$ .

### Possible extensions

In later versions we will aim at introducing

- Addition of x-, y-, and z-translations as well as partly illuminated samples (stripes, grains moving in and out of the beam)
- Additional rotations, such as a tilt below the omega stage.
- More details on flipping
- Inclusion of effects related to beam divergence and energy spread.

## 3. Representation of crystallographic orientation

Crystallographic orientations can be expressed in numerous ways, as described in detail in the literature on texture [5,6]. We will use four representations. For algebra the natural choice is the 3x3 orthogonal matrix  $\mathbf{U}$  or its inverse (transpose)  $\mathbf{g}$ , as defined above. For visualisation and sampling a representation by three parameters is preferable. We have chosen three alternatives: Euler angles, Rodrigues vectors and quaternions. In the following we provide definitions and summarise the most important transforms and geometric properties for each of the representations. A discussion of crystal symmetry will be given in chapter 4.

### Euler angles (Bunge definition)

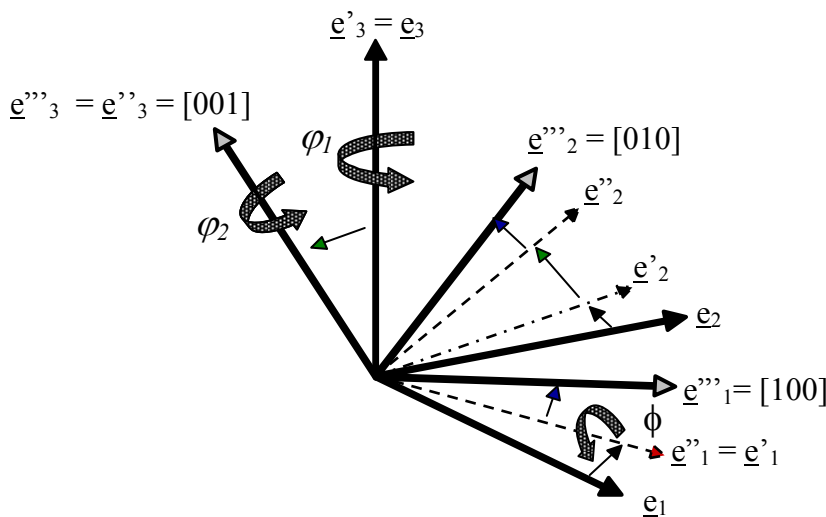


**Figure 3.1**

Definition of the Euler angles ( $\varphi_1, \phi, \varphi_2$ ) according to Bunge [7]. The sample system  $(\underline{e}_1, \underline{e}_2, \underline{e}_3)$  is rotated first around the third axis by  $\varphi_1$ , then around the new first axis  $\underline{e}'_1$  by  $\phi$  and finally around the new third axis  $\underline{e}''_3$  by  $\varphi_2$  to match the Cartesian grain system  $(\underline{e}''_1, \underline{e}''_2, \underline{e}''_3)$ . For cubic systems the latter set is identical to the reciprocal axes ( $[100], [010], [001]$ ).

Traditionally, orientations are parameterized by a set of Euler angles  $(\varphi_1, \phi, \varphi_2)$ , expressing subsequent rotations around three axes, cf. Fig 3.1. With the definitions of the angles as provided by Bunge [7]:

$$U = \begin{bmatrix} c(\varphi_1)c(\varphi_2) - s(\varphi_1)s(\varphi_2)c(\phi) & -c(\varphi_1)s(\varphi_2) - s(\varphi_1)c(\varphi_2)c(\phi) & s(\varphi_1)s(\phi) \\ s(\varphi_1)c(\varphi_2) + c(\varphi_1)s(\varphi_2)c(\phi) & -s(\varphi_1)s(\varphi_2) + c(\varphi_1)c(\varphi_2)c(\phi) & -c(\varphi_1)s(\phi) \\ s(\varphi_2)s(\phi) & c(\varphi_2)s(\phi) & c(\phi) \end{bmatrix} \quad (3.1)$$

Here we have used the shorthands c and s for cos and sin, respectively. The reverse relationship is given by (code is provided in an appendix):

**MISSING** (3.2)

Calculating the combined rotation of two individual rotations is very cumbersome in the Euler angle representation. This should be done using one of the other representations.

*Sampling* Euler space is non-linear with singularities at  $\phi = 0$  and  $\pi$ . In order to sample it uniformly use of the metric  $d\mathbf{g}$  is required [7]

$$d\mathbf{g}(\phi, \varphi_1, \varphi_2) = \frac{1}{8\pi^2} \sin(\phi) d\phi d\varphi_1 d\varphi_2. \quad (3.3)$$

*Projection lines:* From a single diffraction event, only the direction of the scattering vector is probed. Measurements will be invariant to a rotation of the sample around the vector. The set of orientations, which for given  $\underline{y}$  and  $\underline{h}$  fulfils  $\underline{y} = \mathbf{U} \underline{h}$  (cf. Eq 2.10) constitutes a curve in orientation space, the so-called projection line for pole-figure inversion. It is evident from Eq. 3.1 that such lines are curved in Euler space.

### Rodrigues vectors

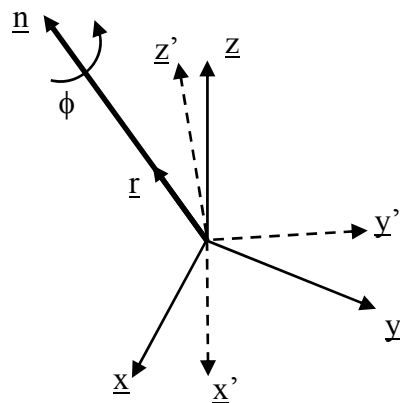


**Figure 3.2**

Definition of the Rodrigues vector  $\underline{r}$ . The coordinate system  $(x,y,z)$  is rotated around  $\underline{n}$  by angle  $\phi$  into  $(x',y',z')$ .  $\underline{r}$  is parallel to  $\underline{n}$ :  $\underline{r} = \underline{n} \tan(\phi/2)$ .

The Rodrigues representation is in several ways more elegant and better suited for numerical work in connection with diffraction data [8-10]. It is based on the fact that any rotation can be represented in a unique way by a rotation axis  $\underline{n}$  and a rotation angle  $\phi$ , defined on  $[0 \pi]$ . In the Rodrigues parameterisation these are coupled in the definition of the Rodrigues vector [11]

$$\underline{r} = \tan(\phi/2)\underline{n}. \quad (3.4)$$

The definition is illustrated in Fig 3.2.

The vector  $\underline{r}$  can be treated as a vector in  $\mathbf{R}^3$ , with the exception of points with a rotation angle of  $\pi$ , which are represented by two opposite points in infinity. The axes of this space are co-linear with those of the sample system in the sense, that a vector  $\underline{r} = (r_1, 0, 0)$  describes a rotation around the sample x-axis.

The relationship to  $\mathbf{g} = \mathbf{U}^{-1}$  is given by<sup>9</sup>

$$g_{ij} = \frac{1}{r^2} \left[ (1 - r^2) \delta_{ij} + 2r_i r_j - 2\varepsilon_{ijk} r_k \right], \quad (3.5)$$

where  $r^2 := r_k r_k$ , and  $\varepsilon_{ijk}$  is the permutation tensor:

$$\varepsilon_{ijk} = \begin{cases} +1 & \text{if } (i, j, k) \text{ is } (1, 2, 3), (2, 3, 1) \text{ or } (3, 1, 2), \\ -1 & \text{if } (i, j, k) \text{ is } (3, 2, 1), (1, 3, 2) \text{ or } (2, 1, 3), \\ 0 & \text{otherwise: } i = j \text{ or } j = k \text{ or } k = i, \end{cases}$$

The reverse relationship (determining  $\underline{r}$  given  $\mathbf{U}$ ) is defined by

$$r_i = \frac{\varepsilon_{ijk} g_{jk}}{1 + g_{mm}}. \quad (3.6)$$

The result  $\underline{r}_3$  of two rotations, first  $\underline{r}_1$  and then  $\underline{r}_2$  is

$$\underline{r}_3 = \frac{\underline{r}_1 + \underline{r}_2 - \underline{r}_1 \times \underline{r}_2}{1 - \underline{r}_1 \cdot \underline{r}_2}$$

*Sampling* The metric  $d_{ij}$  and the volume element  $dV$  are

$$d_{ij} = \frac{1}{(1 + r^2)^2} \left[ (1 + r^2) \delta_{ij} - 2r_i r_j \right]; \quad (3.7)$$

---

<sup>9</sup> In Eqs 3.5 and 3.6 we use Einstein summation rule. That is the sign for summation over vector and tensor suffices is omitted. Summation is understood with respect to all suffices that appear twice in a given term.

$$dV = \sqrt{\det(d_{ij})} = \frac{dr_1 dr_2 dr_3}{1+r^2}. \quad (3.8)$$

Evidently this leads to complications for  $r \rightarrow \infty$  (that is for low crystal symmetry, cf. Chapter 4). On the other hand, for  $\phi \rightarrow 0$  rotations become commutative. This is reflected in the fact that the metric becomes linear. As an example, for orientation distributions characterized by  $\phi < 10$  deg, the space is Euclidean within an accuracy of better than 1%.

*Projection lines* A key fact is that the projection lines for pole-figure inversion are straight lines. Specifically, for a given set of vectors  $\underline{h}$  and  $\underline{y}$ , the projection line is given by

$$\underline{r} = \underline{r}^0 + t \frac{\underline{h} + \underline{y}}{1 + \underline{h} \cdot \underline{y}}; \quad -\infty < t < \infty \quad (3.9)$$

$$\underline{r}^0 = \frac{\underline{h} \times \underline{y}}{1 + \underline{h} \cdot \underline{y}} = \tan\left(\frac{\phi_0}{2}\right) \underline{n}. \quad (3.10)$$

where  $\underline{r}^0$  is the rotation from  $\underline{h}$  into  $\underline{y}$  with the minimum rotation angle  $\phi_0$ . The second term in Eq. 3.7 corresponds to an arbitrary rotation around the symmetric position  $\underline{h} + \underline{y}$ .

For  $\phi \rightarrow 0$  the expression for the projection line simplifies to

$$\underline{r} = \frac{1}{2}(\underline{h} \times \underline{y}) + \frac{t}{2}(\underline{h} + \underline{y}). \quad (3.11)$$

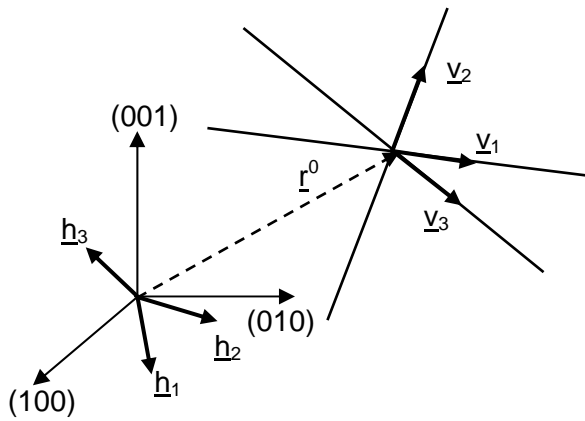


**Figure 3.3.**

Symmetry of projection lines through point  $\underline{r}^0$  in Rodrigues space. The directions of three normalised (h,k,l)-vectors ( $\underline{h}_1$ ,  $\underline{h}_2$ ,  $\underline{h}_3$ ) is marked. The associated projection lines pass through  $\underline{r}^0$  with directions ( $\underline{v}_1$ ,  $\underline{v}_2$ ,  $\underline{v}_3$ ).

As a first application of the Rodrigues vector formalism let us address the question: for a given orientation  $\underline{r}^0$ , what is the geometry of the projection lines observed?

The answer is illustrated in Fig 3.3, where the full Rodrigues space is used. Assume that detection geometry and intensity concerns enable the observation of the set of reflections ( $\underline{h}_1, \underline{h}_2, \dots, \underline{h}_N$ ). Then from Eq. 3.8 it follows that the associated projection lines are straight line passing through  $\underline{r}^0$  with the  $i$ 'th line pointing in the direction

$$\underline{v}_i = \frac{(I + U)\underline{h}_i}{1 + \underline{h}_i U \underline{h}_i}. \quad (3.12)$$

As the expression conserves angles between vectors, the set ( $\underline{v}_1, \underline{v}_2, \dots, \underline{v}_N$ ) is a rotation of the set ( $\underline{h}_1, \underline{h}_2, \dots, \underline{h}_N$ ). In other words the projection lines associated with a given orientation exhibit the underlying crystal symmetry.

### Quaternions

Quaternions and their applications to rotations and orientations have a well-developed theory [12-16]. In this section we give only a skeleton development, restricting our attentions to those definitions and facts that we absolutely need for our purpose.

*Quaternion basics:* A quaternion  $\mathbf{q}$  is a 4-tuple ( $a, b, c, d$ ) of real numbers. The product of two quaternions is defined by

$$(a_1, b_1, c_1, d_1) (a_2, b_2, c_2, d_2) = (a_3, b_3, c_3, d_3), \quad (3.13)$$

where

$$\begin{aligned} a_3 &= a_1 a_2 - b_1 b_2 - c_1 c_2 - d_1 d_2, \\ b_3 &= a_1 b_2 + b_1 a_2 + c_1 d_2 - d_1 c_2, \\ c_3 &= a_1 c_2 - b_1 d_2 + c_1 a_2 + d_1 b_2, \\ d_3 &= a_1 d_2 + b_1 c_2 - c_1 b_2 + d_1 a_2. \end{aligned} \quad (3.14)$$

Multiplication is associative, and so one can use unambiguously the notation  $\mathbf{pqr}$  for the product of the three quaternions  $\mathbf{p}$ ,  $\mathbf{q}$ , and  $\mathbf{r}$ . Note also that  $(1, 0, 0, 0)$  is an identity element; i.e., for any quaternion  $\mathbf{q}$  we have  $(1, 0, 0, 0)\mathbf{q} = \mathbf{q} = \mathbf{q}(1, 0, 0, 0)$ .

The norm of the quaternion ( $a, b, c, d$ ) is defined by

$$|(a, b, c, d)| = \sqrt{a^2 + b^2 + c^2 + d^2}. \quad (3.15)$$

We now specify two useful subsets of the set of quaternions. For both of these it is helpful to introduce the notation  $(a, \mathbf{b})$ , where  $\mathbf{b}$  is the 3D vector  $(b, c, d)$ , to abbreviate the quaternion  $(a, b, c, d)$ . The conjugate of the quaternion  $\mathbf{q} = (a, \mathbf{b})$  is defined to be  $\overline{\mathbf{q}} = (a, -\mathbf{b})$ . The conjugate of the product of two quaternions is the reversed product of their conjugates; i.e.,  $\overline{\mathbf{q}_1 \mathbf{q}_2} = \overline{\mathbf{q}_2} \overline{\mathbf{q}_1}$ .

### *Relation between unit quaternions and orientations:*

The set of unit quaternions consists of quaternions whose norm is 1. These span  $SO(3)$ , the 3-sphere in 4-space, similar to e.g. the Earth surface being a 2-sphere in 3-space. The product of two unit quaternions is a unit quaternion, and that the conjugate of a unit quaternion is also a unit quaternion.

There is a 2-to-1 mapping between unit quaternions and rotations, as specified by angle  $\phi$  and unit direction  $\underline{n}$ :

$$\mathbf{q} = (a, \mathbf{b}) = (\cos(\phi/2), \underline{n} \sin(\phi/2)) \quad (3.16)$$

Note that  $\mathbf{q}$  and  $-\mathbf{q}$  define the same rotation.

A particularly useful and elegant consequence of this approach is that the rotation represented by the unit quaternion  $\mathbf{q}_1$  followed by the rotation represented by the unit quaternion  $\mathbf{q}_2$  is the composite rotation represented by  $\mathbf{q}_2\mathbf{q}_1$ .

It appears that quaternion space is bounded.

It follows from Eqs. 3.4 and 3.16 that there is a gnomonic relationship between Rodrigues vectors and unit quaternions. This implies that one can go forth and back, e.g. for visualisation in Rodrigues space and for calculations in quaternion space. **MISSING: equations for going forth and back to Rodrigues space.**

The relationship to  $\mathbf{U}$  is given by

$$\mathbf{MISSING} \quad (3.17)$$

The inverse relationship (determining  $\mathbf{q}$  given  $\mathbf{U}$ ) is defined by

$$\mathbf{MISSING} \quad (3.18)$$

### *Distance*

Following [17] we define the distance  $d$  between two orientations  $\mathbf{q}_1$  and  $\mathbf{q}_2$  by

$$d(q_1, q_2) = \min_{s_1, s_2 \in S} r(q_1 s_1, q_2 s_2) \quad (3.19)$$

where  $S$  is the set of symmetry rotations given by crystal symmetry – see chapter 4 – and  $r$  is

$$r(q_1, q_2) = 1 - |a_3| = 1 - |\cos(\phi_{12})|. \quad (3.20)$$

In other words, the distance  $d$  is the minimal  $r$  when comparing all permutations of symmetry operations. For computing it is relevant to note that it is sufficient to loop over the symmetry operations once, as we can rewrite (3.17) to be

$$d(q_1, q_2) = \min_{s \in S} r((1, 0, 0, 0), s q_2 \bar{q}_1) \quad (3.19)$$

Usually in the materials science literature, we specify the distance  $d(\mathbf{q}_1, \mathbf{q}_2)$  by the associated angle of disorientation, which is defined as that  $\phi$  in the range  $[0^\circ, 180^\circ]$  for which  $\cos(\phi/2) = 1 - d$ .

### Sampling

Knowing that  $a^2 + b^2 + c^2 + d^2 = 1$ , a discretisation by three parameters is evidently possible. The superior way to do so is not known to the authors. In [17,18] one has chosen to sample in a regular grid over the components  $b$ ,  $c$ , and  $d$  in the interval  $[-1, 1]$  and allowing only values that satisfy  $b^2 + c^2 + d^2 \leq 1$ . This sampling leads to neighbouring voxel elements having misorientations that increases with the distance to  $\mathbf{q} = (1,0,0,0)$ .

### Projection lines

In quaternion space the projection lines become circles. Following [16] the circle for a given set of  $\underline{h}$  and  $\underline{r}$  is defined by (under condition  $\underline{h} \times \underline{r} \neq 0$ ) the two orthogonal unit quaternions  $\mathbf{q}_1$  and  $\mathbf{q}_2$

$$q_1 = \left( \cos\left(\frac{\phi}{2}\right), \frac{\underline{h} \times \underline{r}}{\|\underline{h} \times \underline{r}\|} \sin\left(\frac{\phi}{2}\right) \right); \quad q_2 = \left( 0, \frac{\underline{h} + \underline{r}}{\|\underline{h} + \underline{r}\|} \right) \quad (3.20)$$

where  $\phi$  is defined as the angle between  $\underline{h}$  and  $\underline{r}$ , that is:

$$\|\underline{h} + \underline{r}\| = 2 \cos\left(\frac{\phi}{2}\right). \quad (3.21)$$

With these definitions the circle is

$$C(q_1, q_2) = \{q(t) = q_1 \cos(t) + q_2 \sin(t) : t \in [0, 2\pi]\} \quad (3.22)$$

## 4. Crystal symmetry

In texture literature one introduces both crystal and sample symmetry. For multigrain work – as for single grain work - there is no sample symmetry (or stated differently: the sample symmetry is triclinic).

The crystal symmetry operations associated with a given spacegroup can be found in International Tables of Crystallography, Volume A. The relevant generators have been extracted by calls to the [library ??? \[?\]](#).

The crystal symmetry implies that orientation space is divided into a set of  $N$  equivalent sub-spaces, with  $N$  being the number of rotational symmetries (e.g. 24 for cubic systems). We identify one of these as the *fundamental zone*: the one with superior geometric properties such as orientations space being nearly flat. Typically output from programs should refer to the symmetry equivalent in the fundamental zone.

### Fundamental zone:

The relevant numbers for the Euler representation is given in Table 4.1. Notably, the 3-fold axis in cubic materials does not lead to sub-volumes that have a rectangular shape in Euler space. The Phi-interval listed in the table is the one that generate the smallest rectangular box comprising an irreducible volume.

Bravais class	phi1	Phi	Phi2
Cubic	[0 360]	[54 90]	[0 90]
Tetragonal	[0 360]	[0 90]	[0 90]
Orthorhombic	[0 360]	[0 90]	[0 180]
Hexagonal	[0 360]	[0 90]	[0 60]
Trigonal	[0 360]	[0 90]	[0 120]
Monoclinic	[0 360]	[0 90]	[0 360]
Triclinic	[0 360]	[0 180]	[0 360]

**Table 3.1**

Irreducible part of Euler-space for the seven Bravais classes. From [6].

Rodrigues space: The fundamental zone is centered around (0,0,0).

*MISSING: description of the fundamental zone as function of spacegroup.*

Quaternions: The fundamental zone is centered around (1,0,0,0).

*MISSING: description of the fundamental zone as function of spacegroup.*

Determining the orientation in the fundamental zone:

Given an arbitrary orientation we can determine all the symmetry equivalents. For each of these we derive the matrix  $\mathbf{U}_k$ . We then calculate the misorientation with respect to the Identity matrix, that is the misorientation with respect to the center of the fundamental zone:

$$\beta_k = \cos^{-1}\left(\frac{\text{Tr}(\mathbf{U}_k) - 1}{2}\right). \quad (4.?)$$

Here  $\text{Tr}(\mathbf{U}_k)$  is the trace of  $\mathbf{U}_k$ , that is the sum of the three diagonal elements:

$$\text{Tr}(\mathbf{U}) = U_{11} + U_{22} + U_{33}.$$

The symmetry equivalent with the minimum  $\beta$  is the one representing the fundamental zone.

## References

1. H.F. Poulsen. *Three dimensional x-ray diffraction microscopy*. (Springer, Berlin, 2004)
2. Tomo-book
3. W.R. Busing, H.A. Levy. *Acta Cryst.* (1967). 22, 457
4. W.A. Paciorek, M. Meyer, G. Chapuis. *Acta Cryst.* (1999) **A55**, 543-557.
5. U.F. Kocks, C.N. Tome, and H.R. Wenk. *Texture and Anisotropy* (Cambridge University Press, Cambridge, 1998).
6. V. Randl, O. Engler. *Introduction to texture analysis, Macrotecture, Microtexture and Orientation Mapping*. (Gordon and Breach, London, 2000)
7. H.J. Bunge. *Matematische Methoden der Texturanalyse* (Akademie Verlag, Berlin, 1969).
8. P. Neumann. *Text. Microstruct.* (1991) **14-18**, 53-58.
9. A. Morawiec and D.P. Field. *Phil. Mag. A*, (1996) **73**, 1113-1130.
10. A. Kumar and P.R. Dawson. *Acta Mater.* (2000) **48**, 2719-2736.
11. F.C. Frank. *Metall. Trans. A* (1988) **19**, 403.
12. Altmann, S.L.: *Rotations, Quaternions, and Double Groups*. (Clarendon Press, Oxford, 1986).
13. Conway, J.H., Smith, D.A.: *On Quaternions and Octonions: Their Geometry, Arithmetic, and Symmetry*. (A. K. Peters, Natick, MA, 2003).

14. Kuipers, J.B. *Quaternions and Rotation Sequences* (Princeton University Press, Princeton, 1999).
15. Morawiec, A. *Orientations and Rotations. Computations in Crystallographic Textures*. (Springer, Berlin, 2004).
16. L. Meister, H. Schaeben. *Math. Meth. Appl. Sci.* (2005) **28**,101–126
17. A. Alpers, L. Rodek, H.F. Poulsen, E. Knudsen, G.T. Herman. In: *Advances in Discrete Tomography*, Ed. G.T. Herman, A. Kuba (Birkhäuser, Boston, 2007), pp. 271-302
18. A. Kulshreshtha, G.T. Herman, E. Knudsen, L. Rodek, A. Alpers, H.F. Poulsen. Submitted (2007)

## Appendices

1. Code for deriving Euler angles from U
2. Code for deriving U from Euler angles
3. Code for deriving a Rodrigues vector from U
4. Code for deriving a U from a Rodrigues vector
5. Code for deriving a unit quaternion from U
6. Code for deriving a U from a unit quaternion

## 1. Code for deriving Euler angles from U

```
function phi_vector = u2euler(U)

ph(1)=acos(U(3,3));
if ph(1) < 0.0001
    ph2(1) = atan(U(2,1)/U(1,1))/2.0
    ph1(1) = ph2(1)
    phi1_deg = ph1(1)*180/pi;
    phi_deg = ph(1)*180/pi;
    phi2_deg = ph2(1)*180/pi;
else
    % there is 2 solutions to each of the equations
    ph1(1)=atan(-U(1,3)/U(2,3));
    ph2(1)=atan(U(3,1)/U(3,2));
    ph(2)=2*pi-ph(1);
    ph1(2)=ph1(1)+pi;
    ph2(2)=ph2(1)+pi;

    %the right combination is found by brute-force, using the restriction on phi1
    minsum = 1000;
    for j=1:2
        for k=1:2
            U2 = euler2u(ph1(2)*180/pi,ph(j)*180/pi,ph2(k)*180/pi);
            Udev = abs(U2-U);
            sum1 = sum(sum(Udev));
            if sum1<minsum
                minsum=sum1;
                mj = j;
                mk = k;
            end
        end
    end
    phi1_deg = ph1(2)*180/pi;
    phi_deg = ph(mj)*180/pi;
    phi2_deg = ph2(mk)*180/pi;
end
phi_vector = [phi1_deg phi_deg phi2_deg];
```